Journal of Biomedical Optics 6(1), 41–51 (January 2001)

In vivo autofluorescence spectroscopy of human bronchial tissue to optimize the detection and imaging of early cancers

Matthieu Zellweger
Swiss Federal Institute of Technology (EPFL)
DGR-LPAS, Institute of Environmental Engineering
CH-1015 Lausanne, Switzerland

Pierre Grosjean
CHUV Hospital
ENT Clinic
CH-1011 Lausanne, Switzerland

Didier Goujon
Swiss Federal Institute of Technology (EPFL)
DGR-LPAS, Institute of Environmental Engineering
CH-1015 Lausanne, Switzerland

Philippe Monnier
CHUV Hospital
ENT Clinic
CH-1011 Lausanne, Switzerland

Hubert van den Bergh
Georges Wagnières
Swiss Federal Institute of Technology (EPFL)
DGR-LPAS, Institute of Environmental Engineering
CH-1015 Lausanne, Switzerland

Abstract. We are developing an imaging system to detect pre-/early cancers in the tracheo-bronchial tree. Autofluorescence might be useful but many features remain suboptimal. We have studied the autofluorescence of human healthy, metaplastic and dysplastic/CIS bronchial tissue, covering excitation wavelengths from 350 to 480 nm. These measurements are performed with a spectrofluorometer whose distal end is designed to simulate the spectroscopic response of an imaging system using routine bronchoscopes. Our data provide information about the excitation and emission spectral ranges to be used in a dual range detection imaging system to maximize the tumor vs healthy and the tumor vs inflammatory/metaplastic contrast in detecting pre-/early malignant lesions. We find that the excitation wavelengths yielding the highest contrasts are between 400 and 480 nm with a peak at 405 nm. We also find that the shape of the spectra of healthy tissue is similar to that of its inflammatory/metaplastic counterpart. Finally we find that, when the spectra are normalized, the region of divergence between the tumor and the nontumor spectra is consistently between 600 and 800 nm and that the transition wavelength between the two spectral regions is around 590 nm for all the spectra regardless of the excitation wavelength, thus suggesting that there might be one absorber or one fluorophore. The use of backscattered red light enhances the autofluorescence contrast. [DOI: 10.1117/1.1332774]

Keywords: autofluorescence; lung cancer; early detection; imaging; spectroscopy.

Paper JBO-90058 received Nov. 7, 1999; revised manuscript received Sep. 26, 2000; accepted for publication Sep. 26, 2000.

1 Introduction

Carcinoma of the bronchus is the most common cancer in the western world. In determining the 5 year survival associated with the disease, tumor staging is a very important parameter[1,2] as precancerous (dysplasia) and early cancerous lesions (carcinoma *in situ* and microinvasive carcinoma) are indeed much more successfully treated than invasive cancers.[3] The only method of localizing and delineating such lesions is bronchoscopy. However, the changes occurring during the first stages of the cancerization process make it difficult in most cases for the endoscopist to accurately localize the lesions under white light illumination. Several examples of the use of light-induced fluorescence (LIF) have been proposed for point fluorescence measurements and imaging applications with[4–8] and without[4,9–15] the addition of an exogenous drug to enhance the contrast between the early cancerous lesion and the healthy surrounding area.[16] Because they rely upon the natural fluorescence of the tissues, the latter are termed ''autofluorescence'' methods. Due to the geometry of the bronchi and the behavior of particles in the air flow, it is difficult to homogeneously distribute an inhaled exogenous drug to the bronchial epithelium and it is also difficult to perform point fluorescence measurements. Consequently, no exogenous fluorescent markers or exogenously induced drugs (PPIX) have shown convincing results up to now according to our knowledge. In this paper, we are thus reporting on a study about the autofluorescence of the bronchial tissue. Several experimental[8,17,18] and commercially available systems (Xillix,[10,11] Storz,[19] SAFE-1000 (Pentax),[20]) use autofluorescence to create images of the bronchial tissue. The goal of these systems is to detect and distinguish the precancerous and early cancerous lesions from the healthy surrounding area. To do so, most of these systems excite the autofluorescence with blue and/or violet light and detect the autofluorescence in one,[20] or several spectral regions.[8,10,11,19] However, no systematic optimization work has been reported for the spectral design of these systems. Improvement might be possible by optimizing the domains of excitation and detection wavelengths. We propose here a study of the optimization of the excitation wavelength covering a range of excitation wavelengths from 350 to 480 nm, and the detection spectral ranges to detect and characterize the precancerous and early cancerous lesions by autofluorescence in the tracheobronchial tree. Our choice of a dual range detection method is based on our aim of optimizing an imaging system. At least

Address all correspondence to Dr. Georges Wagnières. Tel: 41-21-693-3120; Fax: 41-21-693-3626; E-mail: georges.wagnieres@epfl.ch

1083-3668/2001/$15.00 © 2001 SPIE

two spectral domains are necessary for efficient contrast enhancement. In fact, due to the tridimensional geometry of the bronchi, both a background and a contrast bearing foreground image are necessary. However, detection over many spectral regions is detrimental to the intensity of the fluorescence detected in each region and is consequently shot-noise limited.

Our measurements of the autofluorescence properties of the bronchial tissue *in vivo* are correlated to the histopathological status of the examined sites. Moreover, our measurements took place at a fixed distance between the tissue and the probe. This characteristic is also based on our goal of optimizing an imaging endoscopic system that probes the tissue from a certain distance.

2 Materials and Methods

2.1 Patients

Forty eight patients were involved in this study (see Table 1) from November 1996 to September 1999. The patients were scheduled for rigid bronchoscopy for screening purposes (positive cytology or primary cancerous lesion in the upper aerodigestive tract). Biopsies were taken in the case of a suspicion of an early cancerous lesion. The LIF measurements were executed during the general anesthesia required by rigid bronchoscopy. For safety reasons, not all patients were measured at all wavelengths. All the measurements reported in Table 1 were biopsy confirmed, hence the number of biopsy sites and the number of patients measured per histopathological status are equal.

2.2 Fluorescence Spectroscopy

Our optical fiber-based spectrofluorometer has been described elsewhere[21] and has only been slightly modified (Figure 1) for this study. In brief, it consists of an excitation source (UXL-75 XE, 75 W high pressure Xenon lamp, Ushio Inc., Japan) whose light is passed through a spectrograph (Chromex 250, Chromex, Albuquerque NM 87107), filtered (filter 1 and 2, see Table 2) and injected into a quartz optical fiber hexagonal bundle (seven fibers, HPSUV300A, Oxford Electronics Ltd., Four Marks, Hants, UK; NA=0.22, 300 μm core diameter). This bundle is then connected to a similar bundle that has been adapted to fit the biopsy channel of a standard flexible bronchoscope (Olympus BF-type 20). Four of the seven fibers are used for the excitation light and the remaining three fibers collect the fluorescence light. The distance between the fiber bundle tip and the tissue to be investigated is kept constant (at 3.5 mm,[22]) by a spacer [Figures 2(a) and 2(b)] in order to detect the same spectroscopic response as an imaging system that does not come into actual contact with the tissue during routine inspection. The excitation wavelength is scanned between 350 nm (it is difficult to obtain enough excitation power below this wavelength with a clinically acceptable setup and shorter wavelengths are too far into the UV range to be compatible with this environment) and 480 nm (above this wavelength, the spectral domain of the ''green'' image becomes too narrow to detect enough fluorescence power—see below for the definition of the green image) (see Table 2) by steps of 10 or 15 nm. The resolution of the excitation is $\pm$10 nm full width at half maximum (FWHM) and the typical excitation power at the distal end of the setup is given in Table 2. The fluorescence is filtered by a long pass filter (filter 3, see Table 2) and dispersed by a spectrograph (Chromex 250, Chromex, Albuquerque, NM 87107) to be detected by a Peltier cooled charge coupled device (CCD) (TE/CCD-256, UV coated, Spectroscopy Instruments GmbH, D-82205 Gilching, Germany). LIF is observed in the

Table 1 Number of patients and of spectra for each excitation wavelength and each pathological status.

Excitation wavelength	Histopathological status	Number of patients	Number of spectra
350 nm	Healthy	9	59
	Inflammation/Metaplasia	3	60
	Dysplasia/CIS	2	21
365 nm	Healthy	15	182
	Inflammation/Metaplasia	3	60
	Dysplasia/CIS	2	20
380 nm	Healthy	8	80
	Inflammation/Metaplasia	3	66
	Dysplasia/CIS	2	18
395 nm	Healthy	8	75
	Inflammation/Metaplasia	3	66
	Dysplasia/CIS	2	15
405 nm	Healthy	34	435
	Inflammation/Metaplasia	14	295
	Dysplasia/CIS	5	61
420 nm	Healthy	23	193
	Inflammation/Metaplasia	13	167
	Dysplasia/CIS	4	33
435 nm	Healthy	21	185
	Inflammation/Metaplasia	13	150
	Dysplasia/CIS	5	41
450 nm	Healthy	26	344
	Inflammation/Metaplasia	13	162
	Dysplasia/CIS	5	67
465 nm	Healthy	14	121
	Inflammation/Metaplasia	12	149
	Dysplasia/CIS	3	24
480 nm	Healthy	13	132
	Inflammation/Metaplasia	8	90
	Dysplasia/CIS	3	27

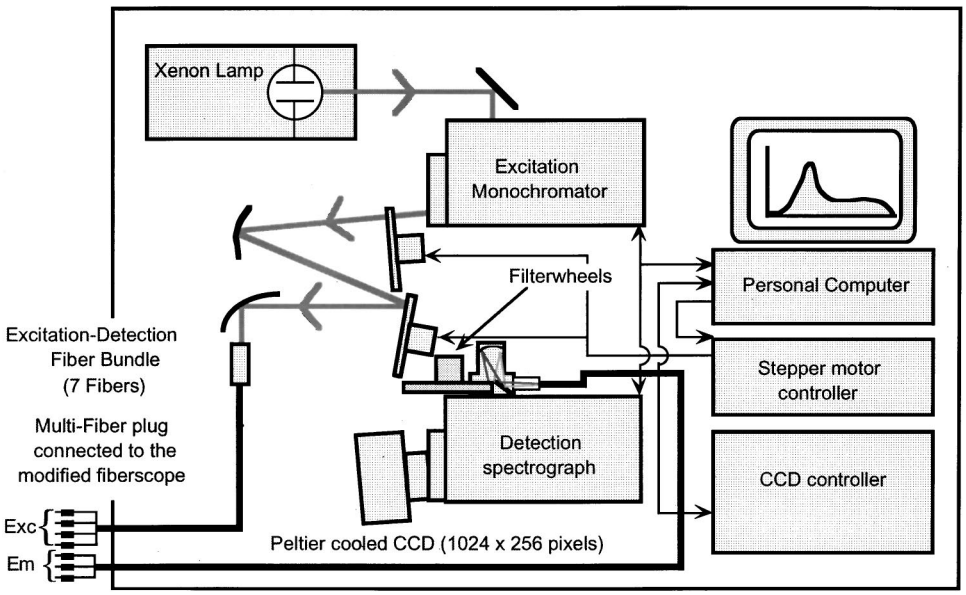

Fig. 1 Apparatus for fluorescence measurements.

Table 2 Characteristics of the filters used for the fluorescence spectroscopy.

Excitation wavelength (FWHM: 20 nm)	Excitation filter (1) (0°)	Dichroic filter (2) (45°)	Emission filter (3) (0°)	Typical power at the distal tip of the probe (±SD)
350 nm (±10 nm)	Bandpass UV, UG5[a]	Dichroic 425 nm, DC425[b]	Longpass 425 nm, FG425[b]	9.2 μW (±2.9 μW)
365 nm (±10 nm)	Bandpass UV, UG5[a]	Dichroic 425 nm, DC425[b]	Longpass 425 nm, FG425[b]	14.9 μW (±4.4 μW)
380 nm (±10 nm)	Bandpass UV, UG5[a]	Dichroic 425 nm, DC425[b]	Longpass 425 nm, FG425[b]	13.8 μW (±4.0 μW)
395 nm (±10 nm)	Bandpass blue, BG3[a]	Dichroic 425 nm, DC425[b]	Longpass 435 nm, FG435[b]	14.2 μW (±4.0 μW)
405 nm (±10 nm)	Bandpass blue, BG3[a]	Dichroic 450 nm, DC450[b]	Longpass 450 nm, FG450[b]	17.7 μW (±4.8 μW)
420 nm (±10 nm)	Bandpass blue, BG3[a]	Dichroic 450 nm, DC450[b]	Longpass 450 nm, FG450[b]	16.4 μW (±5.3 μW)
435 nm (±10 nm)	Dichroic 450 nm, DC450[b]	Dichroic 450 nm, DC450[b]	Longpass 495 nm, FG495[b]	13.7 μW (±4.6 μW)
450 nm (±10 nm)	Dichroic 450 nm, DC450[b]	Dichroic 475 nm, DC475[b]	Longpass 495 nm, FG495[b]	15.6 μW (±6.4 μW)
465 nm (±10 nm)	Dichroic 550 nm, DC550[b]	Dichroic 475 nm, DC475[b]	Longpass 515 nm, FG515[b]	11.5 μW (±3.8 μW)
480 nm (±10 nm)	Dichroic 550 nm, DC550[b]	Dichroic 550 nm, DC550[b]	Longpass 530 nm, FG530[b]	24.4 μW (±4.4 μW)

[a] Filters by Schott Glaswerke, D-55116 Mainz, Germany.

[b] Filters by Reynard, San Clemente, CA 92673-6227.

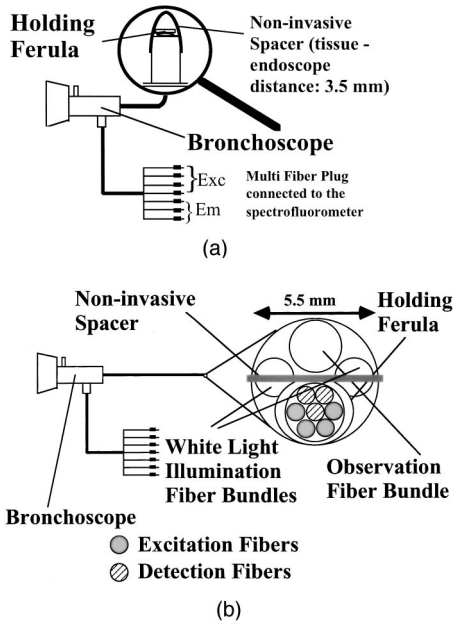

Fig. 2 Probe for calibrated fluorescence spectroscopy [(a) side view; (b) front view].

range between 425 and 800 nm (depending on the excitation wavelength) with a resolution of 11 nm (FWHM). The whole setup is controlled by a 486 PC (Fast 486/50, Spectroscopy Instruments GmbH, D-82205 Gilching, Germany) with CSMA software (Spectroscopy Instruments GmbH, D-82205 Gilching, Germany) and mounted on a trolley for transport to the medical facility. The acquisition time of one spectrum is 2 s.

Before each clinical autofluorescence measurement session, the fluorescence spectrum of an aqueous solution of rhodamine B ($c = 1 \times 10^{-6}$ M) in a 10 mm quartz cuvette is measured. The magnitude of the peak at 575 nm allows for a certain degree of lamp output fluctuations to be taken into account and corrected for. Fluorescence excitation of the rhodamine takes place at each of the excitation wavelengths and detection is between 450 and 800 nm (depending on the excitation wavelength). The fluorescence excitation light power is measured by placing the distal end of the modified bronchoscope into the detector of an optical power meter (Newport Instruments, 840-C). The spectrum of a nonfluorescent tissue-like phantom[23] is also measured. This spectrum is a background spectrum and allows for the subtraction of the fluorescence generated within the optical system (fiber bundle, filters, etc.).

2.3 Correction of the Raw Spectra

The raw spectra are corrected for the spectral response of the detector. This procedure has been described in detail elsewhere.[22] In brief, the spectrum of a calibrated lamp (the spectral emission of which is close to the emission of a perfect blackbody) was acquired with the setup that we used for this study. The resulting curve combined with the measurement of the fluorescence excitation power is used to divide the raw spectra, thus yielding corrected spectra expressed in pW of fluorescence collected by the spectrofluorometer per nm and per μW of excitation power [pW/(μW* nm)]. In our study, this correction yields spectra whose shape is correct, and whose magnitude is correct down to a certain multiplicative factor that in turn depends on the instrumentation that was used. Nevertheless, the spectra throughout this study can be compared between themselves and are therefore expressed in ''relative units'' (r.u.). It should be noted that the measurement of the spectral response of the setup was found to vary little over time and to be consequently of little effect on our results.

2.4 Procedure

After the routine endoscopical observation of the tracheobronchial tree, the modified fiberoscope was passed through the rigid sheath. It was then placed onto the site to be measured. The spacer ensured a gentle contact with the tissue at a fixed distance (3.5 mm) between the fibers and the tissue. This distance was chosen as the best trade-off between the geometrical distortion of the spectra requiring as long a distance as possible and the signal-to-noise-ratio (SNR) decrease requiring as close a distance as possible to minimize the integration time.[22] The endoscopical standard white light illumination was switched off. Ten spectra were recorded on the same location for each excitation wavelength. The endoscopical light was then switched on again. The site was checked for the absence of blood prior to proceeding to further measurements and its macroscopical aspect was recorded. At the end of the measurement session, a biopsy was taken at the site of the measurements to check the histopathology of the site.

2.5 Histological Examination

The biopsies were processed and analyzed in a routine fashion in the Institute of Pathology at the CHUV Hospital. The pathologists reported the results of microscopy and they were assigned to three different groups for the treatment of our spectral data: normal mucosae without any trace of inflammation or metaplasia were grouped under the label ''Healthy.'' Inflammatory or metaplastic mucosae without malignant changes were grouped under the label ''Inflammation/Metaplasia.'' The mucosae bearing pre-/early malignant features (mild, moderate and severe dysplasia as well as carcinoma *in situ*) were grouped under ''Dysplasia/CIS.'' This grouping makes sense as it separates the healthy from the nonhealthy but noncancerous (inflammatory or metaplastic) tissues and from the early cancerous tissues.

2.6 Analysis of Results

2.6.1 *Mean and typical autofluorescence spectra*

The background spectrum of the phantom was subtracted from each measurement. For each set of ten raw spectra at a given site, a mean spectrum was calculated. This mean spectrum was corrected by the rhodamine reference value to correct for some instabilities of our setup. All the mean spectra of a given excitation wavelength were then grouped according to the histopathological status (see above for the classifications) of their corresponding biopsy, normalized and averaged. This yielded three (see Table 1) spectra (thereafter called ''typical'' spectra) for each excitation wavelength (see an example

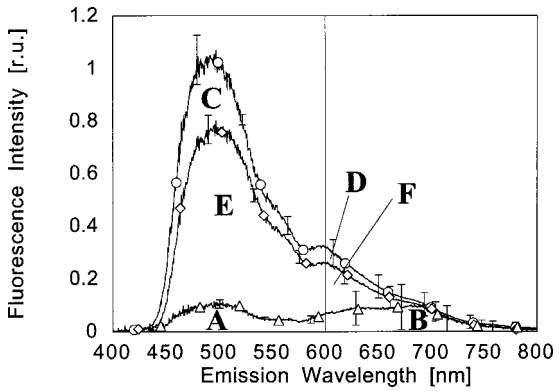

Fig. 3 Typical autofluorescence spectrum of healthy (circles), inflammatory/metaplastic (diamonds), and pre-/early cancerous (triangles) lung tissue excited at 405 nm *in vivo*. The error bars represent the 67% confidence interval and the vertical line is drawn for the separation of the short-wavelength (green) and long-wavelength (red) regions of the spectra. The green region of the healthy spectrum is termed C, of the inflammatory/metaplastic, E and of the pre-/early cancerous, A. Similarly, the red regions are termed D, F, and B.

in Figure 3 for 405 nm as the excitation wavelength). These typical spectra are given for a histopathological status and a standard deviation of the mean was computed (also in Figure 3). They were corrected for the spectral sensitivity of the optical setup and detector (see above or Ref. 22 for the procedure).

2.6.2 *Cut-on wavelength*

The first parameter to determine for the spectral optimization of a dual range detection imaging device is the cut-on wavelength which separates the spectral domains corresponding to the foreground and background images. For this purpose, the typical nonhealthy spectra and the typical healthy spectrum were superimposed (see an example in Figure 4 for 405 nm as the excitation wavelength). The difference between the 'Dysplasia/CIS' and the 'Healthy' typical spectra, or the difference between the Dysplasia/CIS and the Inflammation/Metaplasia typical spectra was calculated (see an example for the difference between the Dysplasia/CIS and the Healthy in Figure 4 for 405 nm as the excitation wavelength). The shortest wavelength corresponding to the half maximum value yielded the ''cut-on'' wavelength (600 nm in Figure 4). This wavelength is used below for the optimization of the sensitivity (Dysplasia/CIS versus Healthy) and the optimization of the specificity (Dysplasia/CIS versus Inflammation/Metaplasia). This separation of the autofluorescence spectra into two regions, namely a short-wavelength region (thereafter ''green'' region) and a long-wavelength region (thereafter ''red'' region) is justified because it has been reported in several papers[7,24] that the decrease of autofluorescence on pre-/early cancerous lesions is larger in the green part than in the red part of the spectrum.

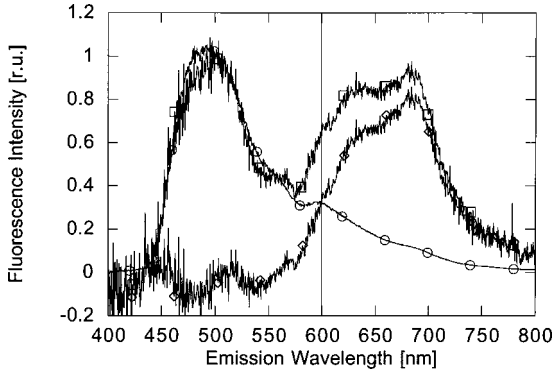

Fig. 4 Superimposed normalized typical autofluorescence spectra of healthy (circles) and pre-/early cancerous (squares) lung tissue excited at 405 nm *in vivo* and difference (diamonds) between the pre-/early cancerous and the healthy spectra. The half maximum of the difference defines the cut-on wavelength and is displayed as a vertical line.

2.6.3 *Sensitivity and specificity*

To optimize the sensitivity and the specificity of our method, we need to compare the typical Dysplasia/CIS spectrum with either the typical Healthy spectrum (sensitivity) or with the typical Inflammation/Metaplasia spectrum (specificity). We named the fluorescence relative power of the green and the red regions of the Dysplasia/CIS spectrum ''A'' and ''B,'' respectively, the fluorescence relative power of the green and the red regions of the Healthy spectrum ''C'' and ''D,'' respectively, and the fluorescence relative power of the green and the red regions of the Inflammation/Metaplasia spectrum ''E'' and ''F,'' respectively (see an example in Figure 3 for 405 nm as the excitation wavelength). A, B, C, D, E, and F were calculated for each measurement whenever the spectra were available. The corresponding R, R', and R'' ratios (see below) were then calculated for each measurement, as well as a subsequent mean R, R', or R'' for the relevant patient. The general mean of these mean ratios is plotted in Figures 6(a), 6(b), and 6(c) as a function of the excitation wavelength.

As stated above, we defined three ratios to quantify the modifications of the spectra associated with different histopathological statuses in order to optimize both the sensitivity (Tumor versus Healthy modifications) and the specificity (Tumor versus Inflammation/Metaplasia modifications), namely R, R', and R'' as

$$R_{\text{Sens.}}=\frac{C}{A}\div\frac{D}{B}=\frac{B\times C}{A\times D}\quad\text{and}\quad R_{\text{Spec.}}=\frac{E}{A}\div\frac{F}{B}=\frac{B\times E}{A\times F},$$

$$R'_{\text{Sens.}}=\frac{C}{A}\quad\text{and}\quad R'_{\text{Spec.}}=\frac{E}{A},$$

$$R''_{\text{Sens.}}=\frac{D}{B}\quad\text{and}\quad R''_{\text{Spec.}}=\frac{F}{B}.$$

These ratios express the ratio of the modifications in the green over the modifications in the red ($R_{\text{Sens.}}$ for the Tumor versus Healthy modifications and $R_{\text{Spec.}}$ for the Tumor versus Inflammation/Metaplasia modifications), the modifications in the green ($R'_{\text{Sens.}}$ for the Tumor versus Healthy modifications and $R'_{\text{Spec.}}$ for the Tumor versus Inflammation/Metaplasia modifications) and the modifications in the red ($R''_{\text{Sens.}}$ for the Tumor versus Healthy modifications and $R''_{\text{Spec.}}$ for the Tumor versus Inflammation/Metaplasia modifications). It should be noted that these ratios are monotonic functions of the Tumor versus Healthy and Tumor versus Inflammation/Metaplasia

contrasts and that R is a monotonic function of the chromatic contrast. It should also be taken into account that R is independent of the tissue-probe distance whereas this is not the case for R' and R''. To optimize the autofluorescence detection method, we need to find the excitation wavelength maximizing one or several of these ratios, depending on the approach that has been chosen.

3 Results

3.1 Typical Autofluorescence Spectra

The typical autofluorescence spectra of the healthy tissue, inflammatory/metaplastic tissue, and dysplasia/CIS excited at 405 nm are presented in Figure 3. The typical spectrum of the healthy tissue is the average of 435 measurements, the typical spectrum of the inflammatory/metaplastic tissue is the average of 295 measurements, and the typical spectrum of the dysplasia/CIS is the average of 61 measurements. The three typical spectra are plotted on the same scale to reflect their relative intensity. The Dys/CIS versus Healthy cut-on wavelength (600 nm) is plotted just for the sake of clarifying the concept, along with the six regions of interest (A, B, C, D, E, and F). The regions at shorter (longer) wavelengths than the cut-on wavelength are named green (red) regions, respectively. The units are relative units as a multiplicative factor, which depends on the geometry of the optical coupling of the fluorescence light into the detection fiber at the distal end of our device, which would intervene to actually have units independent of our spectrofluorometer. The error bars in Figure 3 express the 67% confidence interval.

It should be noted that such typical spectra were measured and computed (see Table 1) for the other excitation wavelengths (350, 365, 395, 420, 435, 450, 465, and 480 nm) but are not displayed for the sake of readability.

It is interesting to note that the Healthy and the Inflammation/Metaplasia typical spectra are very reproducible from one patient to another, hence the small error bars (this was observed at all excitation wavelengths). Moreover, it should be noted that, when superimposed, the Inflammation/Metaplasia typical spectra and the Healthy typical spectra are quite close in shape (data not shown). This feature is especially striking for the excitation wavelength 405 nm: both typical spectra (Healthy and Metaplasia) are overlapped and nearly indistinguishable. This seems to indicate that there is little, if any, difference in the spectral shape of the healthy and the inflammatory/metaplastic lung tissue, whereas the intensity of the latter is significantly smaller than that of the former. Moreover, the small error bars observed on the Inflammatory/Metaplasia typical spectra tend to indicate that this measurement is also highly reproducible. These features are observable for each excitation wavelength (data not shown) and are in agreement with previously reported results.[25]

The error bars of the Dysplasia/CIS typical spectrum are also plotted in Figure 3. They appear to be larger than on the Healthy typical spectrum. This might partly be due to the much smaller statistics (the product of the error bar and the square root of the number of measurements is not constant) and partly to an inherent inhomogeneity of the early cancerous lesions.

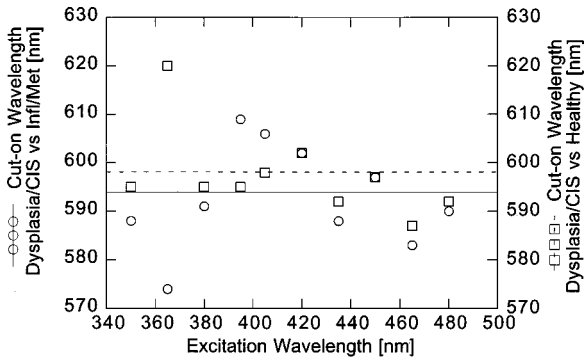

Fig. 5 Cut-on wavelength as a function of the excitation wavelength. The mean cut-on wavelength for the Dysplasia/CIS vs healthy tissues (squares and broken line) and Dysplasia/CIS vs Inflammatory/Metaplastic tissues (circles and plain line) is displayed.

Figure 4 shows the superimposed typical spectra for the healthy tissues and the early cancerous tissues excited at 405 nm. The difference of the two typical spectra is also plotted along with the cut-on wavelength (half maximum).

This calculation was carried out for each excitation wavelength and the results are given in Figure 5 as the cut-on wavelength for the optimization of the sensitivity (Dysplasia/CIS versus Healthy) and the optimization of the specificity (Dysplasia/CIS versus Inflammation/Metaplasia) together with the average cut-on wavelength for both cases. It is interesting to note that the cut-on wavelengths for sensitivity and specificity are very close to each other within an excitation wavelength (with one exception, 365 nm) and also very close to each other from one wavelength to another (again, with the exception of 365 nm) at around 600 nm. It is likely that this reflects a general property of the biological tissue.

The ratios R and R' and R'' are plotted for the optimization of both sensitivity and specificity as a function of the excitation wavelength in Figures 6(a) (R), 6(b) (R'), and 6(c) (R''). Such a graph is intended to provide an answer to the issue of the best excitation wavelength for maximum sensitivity and maximum specificity. The nominal values of R' are larger than those of R because the decrease in the autofluorescence in the green is offset by a smaller decrease of the autofluorescence in the red. The UV excitation wavelengths (350–395 nm) seem to be less efficient in generating a contrast than the blueviolet excitation wavelengths (400–465 nm) and excitation around 405 nm seems to yield the highest contrast. It is also interesting to note that this excitation region seems to hint at the same fluorescence excitation wavelengths for both the optimization of sensitivity and the optimization of specificity. The fact that the ''pure'' decrease in the green (as given by R') is more important than the R ratio is in agreement with the previously stated observation that the autofluorescence decrease is larger in the green than in the red. This is further demonstrated by the fact that R' is almost systematically larger than R''. Consequently, the use of backscattered red light would allow the clinician to take advantage of the whole decrease in the green region (because it would correspond in our case to $R''=1$ or $R=R'$) without the offset of the modifications of the red autofluorescence.

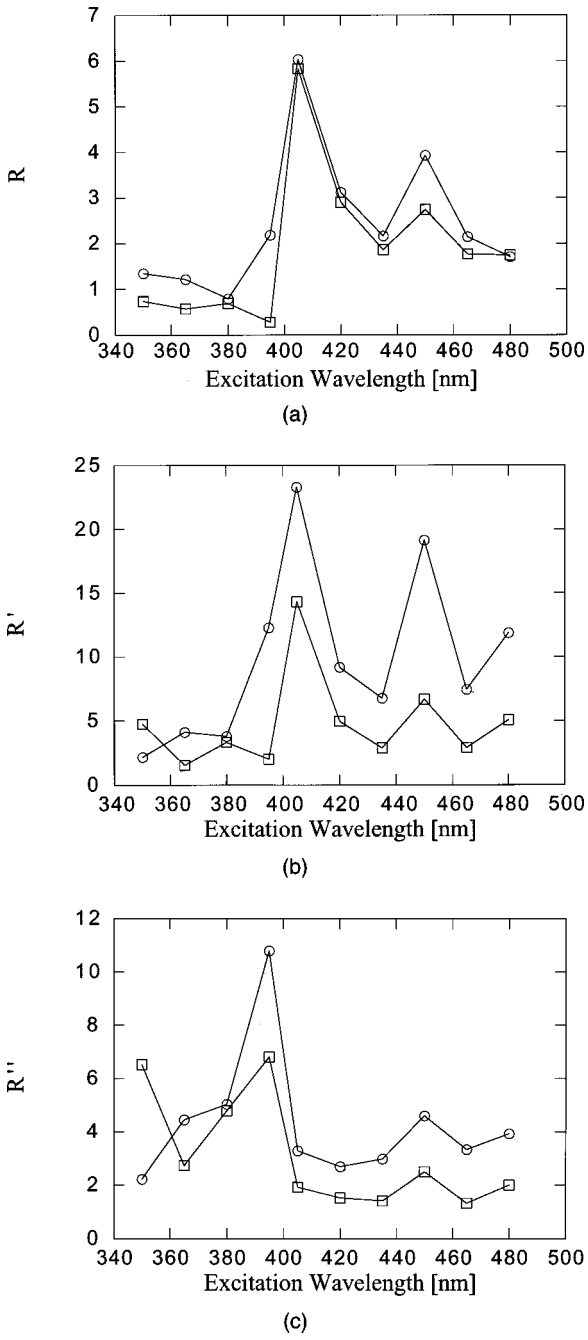

Fig. 6 Ratios $R_{Sens.}$ [(B*C)/(A*D), Dysplasia/CIS vs Healthy, circles] and $R_{Spec.}$ [(B*E)/(A*F), Dysplasia/CIS vs Inflammatory/Metaplastic, squares] as a function of the excitation wavelength (a). Ratios $R'_{Sens.}$ (C/A, Dysplasia/CIS vs Healthy, circles) and $R'_{Spec.}$ (E/A, Dysplasia/CIS vs Inflammatory/Metaplastic, squares) as a function of the excitation wavelength (b). Ratios $R''_{Sens.}$ (D/B, Dysplasia/CIS vs Healthy, circles) and $R''_{Spec.}$ (F/B, Dysplasia/CIS vs Inflammatory/Metaplastic, squares) as a function of the excitation wavelength (c).

4 Discussion

Since the first ''blue light endoscopies'' by Hürzeler,[26] much has been learned about the fluorescence techniques applied to detect early cancerous lesions of the bronchi. Several commercial systems have been built and tested throughout the world. However, no optimization study preceded these developments.[27–30] Such a study could lead to significant improvements in future photodetection systems. A possible way to contribute to this improvement is to optimize the spectral designs of the systems. To do so, a study of the excitation wavelengths and the detection windows was necessary over a large range of excitation wavelengths. This was the main goal of our work. Bearing this goal in mind, we decided to consider a dual range detection method. It is possible to imagine detection algorithms with many channels as has been done for the detection of early lesions in the cervix[31] but this method works fine for point spectroscopic measurements only. For real-time imaging purposes in the tracheo-bronchial tree, the intensity of the fluorescence signal in each detection region also has to be considered. Increasing the number of detection regions will decrease the number of photons in each region. This will eventually be detrimental to the quality of the images that are to be detected.

Several papers report a sharp autofluorescence decrease on early cancerous lesions around 500 nm and/or a relatively less important decrease after 600 nm when excited between 400 and 450 nm.[7,9,32] This is the fundamental base behind all the autofluorescence imaging systems. The Pentax system works with a single range detection principle,[20] whereas a multiple range approach has been preferred for the Xillix and the Storz systems[19,32] and some laboratory systems.[8,17,18] It is interesting to note that our results are in good agreement with these previous results. Indeed, we also found that the autofluorescence of the early cancerous lesions sharply decreases when excited in the blue-violet range and decreases less significantly in the red region. The comparison of the typical spectra takes place through their superimposition, a method that has been used by other groups.[7,25]

The first computation that was performed with the typical spectra was the determination of the cut-on wavelength. From its definition, this is the wavelength that delineates the green and the red regions. In the perspective of a dual range detection system, this would correspond to the transition wavelength of a dichroic mirror. This cut-on wavelength was found to be around 595–600 nm with no measurable dependence on the excitation wavelength. Moreover, the cut-on wavelength for the optimization of sensitivity and for the optimization of specificity were found to be similar. This result seems to indicate that the choice of an excitation wavelength should have little, if any, impact on the spectral specifications of a dichroic mirror. This observation is fortunate for possible future developments of novel photodetection devices. Indeed, it means that the spectral transition yielding the highest sensitivity is the same as the one yielding the highest specificity. The design of such a system could therefore avoid a trade-off between those two concepts. Moreover, this observation seems to hint at the fact that only one class of fluorophores or only one class of absorbers are involved in the modifications of the shape of the autofluorescence spectra.

The previously mentioned observation that the overall autofluorescence decreases between a healthy bronchial tissue and an early cancerous lesion dictated our approach for the treatment of the data. Having defined the green and the red regions of both the healthy and the early cancerous typical spectra, we compared their surfaces. The R ratio takes into account the modifications of the green autofluorescence and the modifications of the red autofluorescence. Since these

modifications seem to be different for both regions (hence the relative ''increase'' in the red region when the typical spectra are superimposed), this is used to generate a color contrast in a dual range detection method. However, the use of the modifications in the red region partly offsets the decrease in the green region (as can be seen with the R' ratio that is larger than the R ratio). This decrease can then be used at its maximum with a single range detection method, but it then loses the advantage of the endoscope-tissue distance independence and is subject to artefacts since it does not rely on two images anymore. This is the trade-off that faces future developers of autofluorescence imaging systems. Another method to avoid this problem is to be found in the use of reflectance light (which, in our case, corresponds to $D=B$ for red reflected light, in which case $R=R'$). Assuming the level of backscattered light does not depend on the tissue-probe distance, it is possible to use the whole range of the decrease in the green region of the spectra. This has been implemented in at least one commercial system with blue backscattered light[19] and has been reported with red backscattered light in the gastrointestinal (GI) tract by Weiss et al.[33]

The superimposition of the typical spectra yields interesting information about the modification of the spectral shape along the cancerization process. The ultimate goal of photodetection is to unequivocally separate the precancerous and early cancerous lesions from the healthy and metaplastic/inflammatory mucosae. Since we chose a dual range detection mode, this means that the shape of the spectra should be such that the modifications in one window are different from the modifications in the other window in a Dysplasia/CIS only and not on metaplastic/inflammatory tissue. It also means that the shape of the spectra for the healthy mucosae and the inflammatory/metaplastic mucosae should be similar enough to be assigned to the same subgroup of noncancerous spots. According to this study, it is very striking that the spectra for the inflammatory/metaplastic tissue often overlap the spectra for the healthy tissue to a large extent. Moreover, the error bars are small on these spectra ($\pm 8.5\%$ on average between 500 and 700 nm for the typical spectrum of healthy tissue excited at 405 nm), thus indicating not only a striking similarity between the spectra of the inflammatory/metaplastic and healthy tissue but also a stable similarity, hence a very high degree of interpatient reproducibility of our measurements. This is in good agreement with results reported by others about the similarity of the spectra acquired on healthy and on inflammatory bronchial tissue.[25] These features tend to indicate that the implementation of this method into an optimized imaging system could yield few false positive results as the inflammatory or metaplastic areas would be consistently similar to the healthy ones.

A more sensitive issue is the stability of the spectral shape of the precancerous/early cancerous areas. Because they are frequently invisible to the naked eye, these lesions are hard to find and hence the possible measurement sites are few. Some excitation wavelengths yield a more important contrast between these lesions and healthy tissue than others, as can be seen in Figure 6(a). The contrast seems to be building up at 395 nm, stays high for blue excitation wavelengths (405–450 nm), and goes down again after 450 nm. This clearly speaks for blue-violet excitation wavelengths instead of UV or longer wavelength light. This observation seems to be consistent whatever the ratioing method [see Figures 6(a), 6(b), and 6(c)]. A non-negligible problem is the large error bars on the Dysplasia/CIS typical spectra (a fact that is observed at each excitation wavelength). Part of the reason behind this fact is the smaller number of measurements on such locations. Nevertheless, most of it might also be due to a naturally higher inhomogeneity of the pre-/early cancerous lesions. Still, at least one other reason should be considered, namely the sampling error, either the fluorescence measurements or the biopsy taking. If a measurement and a biopsy are from different sites, a suspicious-shaped spectrum could be included in the healthy group of spectra or, vice versa, a possibility that would be more detrimental to our study because of the very much smaller number of proven suspicious areas. Although very difficult to prove, such an error could obviously bear heavily on the error bars if found to be true. It is likely, though, that this could easily happen. Indeed, the pre-/early cancerous lesions that we measured were very small patches of diseased cells surrounded by mainly healthy mucosa. In such a situation, one could easily imagine that the shifting of the biopsy forceps by say 1 mm could lead to the sampling of a normal tissue area, whereas the measured spectrum indicated the opposite. As a matter of fact, the smaller statistics of the Dysplasia/CIS group of spectra is not a sufficient reason to explain the larger noise on these measurements (the product of the error bar and the square root of the number of measurements is not constant). This observation clearly speaks in favor of a non-negligible sampling error.

A major drawback of our method would be the instability of the autofluorescence measurements. It is obvious that not only two normal mucosae in two different patients should yield a similar autofluorescence spectrum (interpatient variations of the spectra), but also that several normal sites in the bronchi of the same patient should yield a similar spectrum (intrapatient variations of the spectra). Moreover, if the autofluorescence method were to be used in a routine fashion to detect early cancerous lesions, it should also be able to discriminate between malignant lesions and bruised or irritated mucosae. To study this issue, we therefore measured six autofluorescence spectra on three healthy sites in the bronchi of five patients. We included in these measurements such areas that were normal but macroscopically different (such as erythroplasic/bruised (four), leucoplasic (two), thickened (one) areas). The typical spectra are very similar from one patient to another (interpatient similarity) and very similar to each other (intrapatient similarity) as can be seen from the small error bars in Figure 7 (data for one patient, data from the other patients not shown for the sake of readability). An example of these results is given in Figure 7. The areas measured for Figure 7 are both healthy but differ in their macroscopic aspect. The second spot is reddish (bruised).

It is interesting to note that this result tends to demonstrate that the macroscopic aspect of a normal area in the bronchi is of little influence on the shape of the autofluorescence spectra. This is reassuring as the opposite would mean that the method is close to useless to the clinician. This also demonstrates that the autofluorescence measurements have a good intrapatient stability in addition to a good interpatient stability. This is in agreement with previously published data.[7] This is reassuring as to the possibility of optimizing an imaging photodetection apparatus as it means that these benign lesions would not be

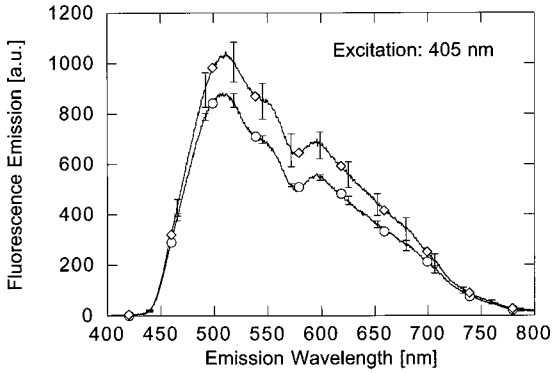

Fig. 7 Measured mean spectra (six measurements each) of the autofluorescence of two spots [both normal: one with a normal appearance (circles) and one bruised (diamonds)] in the bronchi of the same patient. Excitation wavelength: 405 nm.

positive on the autofluorescence images and would also be stable against intrapatient variability.

Such a study over hundreds of spectra can provide knowledge not only about the spectroscopy of early lesions but also about nonmalignant tissues. Clearly, a detection method that yielded a positive result for metaplasias would prove quite useless to the clinician. It is therefore of crucial importance to find a way to assign both the healthy tissues and the nonhealthy but benign (namely the inflammatory and metaplastic tissues) to the same group unequivocally. This means that the spectra should be as stable as possible. Our results tend to show that this is the case.

The use of autofluorescence as a detection method for pre-/early cancerous lesions has been reported in several organs. In the lungs, the most often described system is the LIFE system. This system relies on a dual range detection method.[10] It is recognized as a valuable complement to the standard white-light bronchoscopy.[11,12,34,35] The results behind the development of this system by Hung et al.[9] and Palcic et al.[32] are confirmed by our findings that the fluorescence of the pre-/early cancerous lesions are reduced by around one order of magnitude in the green region with respect to healthy tissue, whereas the decrease is less marked in the red region. As for the modifications of the spectral shape, the authors did not observe any of them for excitation wavelengths of 405 or 442 nm.[9] Still, the decrease in the region around 500 nm is in agreement with their results. In a study about the autofluorescence of bronchial tissue, Qu et al.[25] also report a decrease in autofluorescence intensity between healthy and inflamed tissue as well as between healthy and CIS tissue. They also report that the shape of the spectra of inflamed tissue is similar to that of the spectra of healthy tissue, a result that is confirmed by our findings. However, these authors do not report any modification of the spectral shape of the CIS with respect to the healthy tissue. On the contrary, they show that when their intensity is adjusted accordingly, the spectra of both the healthy tissue and the CIS overlap. Our results are in disagreement with this finding and it is probably a sign that the controversy is still going on as to the exact reasons behind the modifications of the autofluorescence spectra. It should be noted, though, that these authors performed their measurements with a probe in contact with the tissue. It is a critical point as such a measuring procedure only allows a very small volume of tissue to be probed. A possible element of explanation might be that the modifications to the intensity of the autofluorescence spectra might be due to some modifications to the contents in biomolecules (flavins) in the tissue, a feature that is observed by both Qu et al.[25] and ourselves. On the other hand, the modifications in the shape of the autofluorescence spectra might be linked to a deeper lying effect (such as maybe an increase of the relative vascular volume, hence an increase in the relative hemoglobin contents) which would be probed only when observing the tissue from a certain distance. This might be an element of explanation for the discrepancy between the work of these authors and ours. Indeed, the large peak on Figure 6(a) could be reminiscent of a similar peak on the absorption spectrum of hemoglobin.

As an extension of the studies on the Xillix system, Takehana, Kaneko, and Mizuno[36] found that it could be useful in the GI tract and report autofluorescence spectra similar to ours in normal and precancerous tissues in the esophagus. Again, the behavior of the autofluorescence is a decrease on moderate dysplasia and a modification of the spectral shape, in this work a relative increase of the red (580+ nm) contribution. Although this is reported for a different organ, it is interesting to note the striking similarity to our results. Another interesting extension of the Xillix system is reported by Weiss et al.[33] for the esophagus and stomach. In this work, the authors used a fluorescence/reflectance mode by means of red backscattered light. They report an improved contrast with the latter with respect to the former. This corresponds to our R' ratio (because in this case B=D which is the desired effect when adding red reflectance light) and our results are also in agreement with these findings [Figure 6(a)]. The reflectance mode has also been used in the Storz system but this time blue instead of red light is detected.[19] The Storz system was used in a clinical context by Häussinger et al.,[14] who report a similar decrease in the autofluorescence on severe dysplasia with respect to normal epithelium when excited in the 380–460 nm range. The spectral shape of their measurements is not investigated in great detail but their assumption that the color of pre-/early cancerous lesions will be different is a hint that the spectral shape could change. It is indeed the case in the spectra they report, although only one spectrum for each pathological status is given. The blue backscattered light is intended to yield a constant distance-independent background image for dual range detection. Nevertheless, the strong absorption of the blood in this part of the spectrum could cause benign small bruised areas to appear red and thus generate a false positive site.

Another commercially available system that relies on autofluorescence to detect pre-/early cancerous lesions is the SAFE-1000 system. This system uses a single range detection method in the green region of the autofluorescence spectrum. It corresponds to our R' ratio. In such a system, the positive-looking sites appear darker than the surrounding mucosa rather than having a different color.[20] Kakihana et al. report of a clinical study with this system[13] and report a similar decrease in the autofluorescence of an invasive squamous cell carcinoma (excitation at 440 nm) with a relative increase in the fluorescence emission above 540 nm. However, these authors also report that the thickening of the epithelium because of chronic inflammation induces false negative results. More-

over, such a single range system is subject to difficulties due to the fact that the tridimensional geometry of the bronchi induces darker areas that are not lesions but rather areas at a greater distance from the source. The inhomogeneity of the illumination could possibly induce false positive results in a single range system.

There is a recurrent controversy about the reasons of the decrease of the autofluorescence in the green region of the spectrum. A possible explanation is that the fluorescence is reabsorbed by the thickened epithelium (architectural effect). This is a partial explanation proposed by Qu et al.[25] who report interesting changes in intensity of the autofluorescence spectra and parallel changes in the mean thickness of the bronchial epithelium from 46 ± 3 μm in normal epithelium, to 70 ± 7 μm in a dysplasia to 116 ± 16 μm for CIS. However, they do not provide any thickness measurement for the inflammatory tissues, shown in their work to undergo a similar intensity decrease. The epithelial thickening is also invoked by other authors[14] to explain the changes in the autofluorescence emission from pre-/early cancerous tissues. Another possible explanation is a change in the microenvironment (pH, cell metabolism, redox state of the flavins, or the nicotinamides), namely a biochemical effect. Several authors invoke this possibility,[9,37,38] but the clear-cut unequivocal reason behind the changes in autofluorescence emission remains unclear.

In the light of our results, it seems that an architectural effect alone is unlikely. If this were the case, we would observe a continuous change of the autofluorescence spectrum from that of the healthy tissue towards that of the carcinoma *in situ* (namely a gradual spectroscopic change following the gradual thickness change from healthy to metaplasia to dysplasia to CIS). Consequently, we would observe a continuous change in the intensity of the spectrum (actually observed) and a continuous change in the shape of the spectrum (not observed as the inflammatory/metaplastic tissues exhibit the same spectral shape as the healthy tissues). It might well be that the thickening of the epithelium along the process of cancerization is not the only reason that accounts for the modifications to the spectroscopy of the biological tissues during cancerization.

On the other hand, if the modifications were due to biochemical effects only, it is likely that one would observe no change in the autofluorescence spectrum, neither in its shape nor in its intensity, between those of the healthy tissue and the metaplasia, since both are considered normal and nonmalignant. As a matter of fact, we do not observe a change in the spectral shape of the spectra but it is clear that the metaplastic tissues exhibit less fluorescence when excited in the violet-blue region. These elements seem to give us a hint that the modifications in fluorescence are probably not due to one clear-cut reason alone but rather to a group of changes.

The sampling error proved to be a possible problem. When probing a tissue, it might be difficult to take a biopsy at the exact place where the measurements took place. Although this might lead to a spectrum being assigned to the wrong group, it is a negligible problem regarding the typical spectra of healthy tissue. As a matter of fact, the number of stable reproducible spectra that we measured on healthy or metaplastic tissue is such that it allows a small number of possibly wrong measurements to be disregarded. However, such an argument is invalid for the early lesions group of spectra. Due to the relatively small number of lesions, one wrongly assigned spectrum can bear quite heavily on the statistics. Moreover, due to the difficulty of actually seeing these lesions, it is likely that the possible error in the biopsy taking (as well as in the histopathological analysis) could be higher for pre-/early cancerous lesions than for the normal mucosa. Unfortunately, it is hard to imagine any way to overcome such a possible error, especially since small early lesions are surrounded by much larger areas of healthy mucosa.

One goal of the clinician is to clearly separate the tissues that present some malignant change from the tissues that do not (specificity). In this sense, they require some methodology that would assign healthy, inflammatory, and metaplastic tissues to the same group and light and moderate and severe dysplasias as well as carcinoma *in situ* to another group. Our results seem to show that this is the case for spectroscopic measurements. Obviously, there is much more variability from one spectrum to another in the Dysplasia/CIS group than in the Healthy and Metaplasia groups. This is probably due to a much wider range of possible alterations of the tissue. A further similar study could benefit greatly from the investigation of light or moderate or severe dysplasias only. Classifying the spectra of these lesions in three subgroups instead of grouping them into only one category would yield the spectra of all the tissue stages along the cancerization process. However, due to the aforementioned difficulties, great care will have to be exercised when collecting the data.

Our study also yields very interesting results about healthy tissues. They clearly show that there might be something like a typical spectrum for both absolutely healthy bronchial tissue *in vivo* and metaplastic or inflammatory tissue. Moreover, it seems that the spectral shape of these two typical spectra are similar and that they are reproducible. The interpatient and intrapatient fluctuations seem negligible, as can be seen on the error bars of the typical spectra. Such an observation is of great importance not only for developers of future autofluorescence imaging systems but also for clinicians that will eventually use them as it suggests a low level of false positive results.

Acknowledgments

The authors gratefully acknowledge support from the Swiss National Fund for Scientific Research, Grant No. 20-50691.97 and 21-43507.95, the Swiss Priority Program in Optics (PPO II), the ''CHUV-EPFL-UNIL'' Fund for collaboration in the area of biomedical technology, the ''Fonds de Service'' and ''Fonds de Perfectionnement'' of the ENT, Head and Neck Surgery Department at the CHUV Hospital.

References

1. R. Souhami and J. Tobias, *Cancer and its Management*, Blackwell Science, Oxford (1995).
2. S. Lam and H. Becker, ''Future diagnostic procedures,'' *Thoracic endoscopy* **6**, 363–380 (1996).
3. P. Norwell, ''Mechanisms of tumor progression,'' *Cancer Res.* **46**, 2203–2207 (1986).
4. S. Lam, J. Hung, and B. Palcic, ''Detection of lung cancer by ratio fluorimetry with and without Photofrin II,'' *Proc. SPIE* **1201**, 561–568 (1990).
5. R. Baumgartner, R. M. Hubber, H. Schultz, H. Stepp, K. Rick, F. Gamarra, A. Leberig, and C. Roth, ''Inhalation of 5-aminolevulinic

acid: A new technique for fluorescence detection of early stage lung cancer,'' *J. Photochem. Photobiol., B* **36**, 169–174 (1996).
6. Y. Hayata, H. Kato, and J. Ono, ''Fluorescence fiberoptic bronchoscopy in the diagnosis of early stage lung cancer,'' in *Recent Results in Cancer Research*, pp. 121–130, Springer, Berlin (1982).
7. D. J. Anthony, A. E. Profio, and O. J. Balchum, ''Fluorescence spectra in lung with porphyrin injection,'' *Photochem. Photobiol.* **49**, 583–586 (1989).
8. G. Wagnières, A. Studzinski, D. Braichotte, P. Monnier, C. Depeursinge, A. Châtelain, and H. van den Bergh, ''Clinical imaging fluorescence apparatus for the endoscopic photodetection of early cancers by use of Photofrin II,'' *Appl. Opt.* **36**, 5608–5620 (1997).
9. J. Hung, S. Lam, J. C. LeRiche, and B. Palcic, ''Autofluorescence of normal and malignant bronchial tissue,'' *Lasers Surg. Med.* **11**, 99–105 (1991).
10. S. Lam, C. MacAulay, J. Hung, J. LeRiche, A. E. Profio, and B. Palcic, ''Detection of dysplasia and carcinoma *in situ* with a lung imaging fluorescence endoscope device,'' *J. Thorac. Cardiovasc. Surg.* **105**, 1035–1040 (1993).
11. S. Lam, T. Kennedy, M. Unger, Y. E. Miller, D. Gelmont, V. Rusch, B. Gipe, D. Howard, J. C. Leriche, A. Coldman, and A. F. Gazdar, ''Localization of bronchial intraepithelial neoplastic lesions by fluorescence bronchoscopy,'' *Chest* **113**, 696–702 (1998).
12. N. Ikeda, H. Honda, T. Katsumi, T. Okunaka, K. Furukawa, T. Tsuchida, K. Tanaka, T. Onoda, T. Hirano, M. Saito, N. Kawate, C. Konaka, H. Kato, and Y. Ebihara, ''Early detection of bronchial lesions using lung imaging fluorescence endoscope,'' *Diagnostic and therapeutic endoscopy* **5**, 85–90 (1999).
13. M. Kakihana, K. K. Il, T. Okunaka, K. Furukawa, T. Hirano, C. Konaka, H. Kato, and T. Ebihara, ''Early detection of bronchial lesions using system of autofluorescence endoscopy (SAFE) 1000,'' *Diagnostic and therapeutic endoscopy* **5**, 99–104 (1999).
14. K. Häussinger, F. Stanzel, R. M. Huber, J. Pichler, and H. Stepp, ''Autofluorescence detection of bronchial tumors with the D-Light/AF,'' *Diagnostic and therapeutic endoscopy* **5**, 105–112 (1999).
15. S. Lam, C. MacAuley, and B. Palcic, ''Detection and localization of early lung cancer by imaging techniques,'' *Chest* **103**, 12S–14S (1993).
16. G. Wagnières, W. Star, and B. Wilson, ''*In vivo* fluorescence spectroscopy and imaging for oncological applications,'' *Photochem. Photobiol.* **68**, 603–632 (1998).
17. D. R. Doiron, A. E. Profio, R. G. Vincent, and T. J. Dougherty, ''Fluorescence bronchoscopy for detection of lung cancer,'' *Chest* **76**, 27–32 (1979).
18. A. E. Profio and D. R. Doiron, ''A feasibility study of the use of fluorescence bronchoscopy for localization of small lung tumors,'' *Phys. Med. Biol.* **22**, 949–957 (1977).
19. M. Leonhard, ''New incoherent autofluorescence/fluorescence system for early detection of lung cancer,'' *Diagnostic and therapeutic endoscopy* **5**, 71–75 (1999).
20. R. Adachi, T. Utsui, and K. Furusawa, ''Development of the autofluorescence endoscope imaging system,'' *Diagnostic and therapeutic endoscopy* **5**, 65–70 (1999).
21. M. Zellweger, P. Grosjean, G. Wagnières, P. Monnier, and H. van den Bergh, ''Stability of the fluorescence measurement of Foscan® in the normal human oral cavity as an indicator of its content in early cancers of the esophagus and bronchi,'' *Photochem. Photobiol.* **69**, 605–610 (1998).
22. M. Zellweger, D. Goujon, M. Forrer, H. van den Bergh, and G. Wagnières, ''Absolute autofluorescence spectra of healthy bronchial tissue *in vivo*,'' *Appl. Op.* (submitted).
23. G. Wagnières, S. G. Cheng, M. Zellweger, N. Utke, D. Braichotte, J.-P. Ballini, and H. E. van den Bergh, ''An optical phantom with tissue-like properties in the visible for use in PDT and fluorescence spectroscopy,'' *Phys. Med. Biol.* **42**, 1415–1426 (1997).
24. J. Dhingra, D. Perrault, K. McMillan, E. Rebeiz, S. Kabani, R. Manoharan, I. Itzkan, M. Feld, and S. Shapshay, ''Early diagnosis of upper aerodigestive tract cancer by autofluorescence,'' *Arch. Otolaryngol. Head Neck Surg.* **122**, 1181–1186 (1996).
25. J. Qu, C. MacAulay, S. Lam, and B. Palcic, ''Laser-induced fluorescence spectroscopy at endoscopy: Tissue optics, Monte-Carlo modeling and *in vivo* measurements,'' *Opt. Eng.* **34**, 3334–3343 (1995).
26. D. Hürzeler, ''Blue light endoscopy,'' *Laryngoscope* **85**, 1374–1378 (1975).
27. J. M. Kurie, J. S. Lee, R. C. Morice, G. L. Walsh, F. R. Khuri, A. Broxson, J. Y. Ro, W. A. Franklin, R. Yu, and W. K. Hong, ''Autofluorescence bronchoscopy in the detection of squamous metaplasia and dysplasia in current and former smokers,'' *J. Natl. Cancer Inst.* **90**, 991–995 (1998).
28. P. J. M. George, ''Fluorescence bronchoscopy for the early detection of lung cancer,'' *Thorax* **54**, 180–183 (1999).
29. M. Zargi, L. Smid, I. Fajdiga, B. Bubnic, J. Lenarcic, and P. Oblak, ''Laser-induced fluorescence in diagnostics of laryngeal cancer,'' *Acta Oto-Laryngol.* **S527**, 125–127 (1997).
30. M. Dal Fante, ''Diagnostica endoscopica in fluorescenza della displasia e del CIS bronchiale,'' *http://www.villaggiodellasalute.com/&Na/sem-2/dalfante.htm* (1999).
31. N. Ramanujam, M. F. Mitchell, A. Mahadevan, S. Thomsen, A. Malpica, Th. Wright, N. Atkinson, and R. Richards-Kortum, ''Development of a multivariate statistical algorithm to analyze human cervical tissue fluorescence spectra acquired *in vivo*,'' *Lasers Surg. Med.* **19**, 46–62 (1996).
32. B. Palcic, S. Lam, J. Hung, and C. Mac Aulay, ''Detection and localization of early lung cancer by imaging techniques,'' *Chest* **99**, 742–743 (1991).
33. A. A. Weiss, H. Zeng, R. W. Kline, C. Macauley, and N. Mackinnon, ''Use of endoscopic autofluorescence imaging in diagnosis of disease of the esophagus and stomach,'' *Gastrointest Endosc.* **47**, 70–70 (1998).
34. B. Kulapaditharom and V. Boonkitticharoen, ''Laser-induced fluorescence imaging in localization of head and neck cancers,'' *Ann. Otol. Rhinol. Laryngol.* **107**, 241–246 (1998).
35. B. Venmans, T. van Boxem, E. Smit, P. Postmus, and T. Sutedja, ''Results of two years experience with fluorescence bronchoscopy in detection of preinvasive bronchial neoplasia,'' *Diagnostic and Therapeutic Endoscopy* **5**, 77–84 (1999).
36. S. Takehana, M. Kaneko, and H. Mizuno, ''Endoscopic diagnostic system using autofluorescence,'' *Diagnostic and Therapeutic Endoscopy* **5**, 59–63 (1999).
37. Y. Yang, Y. Ye, F. Li, Y. Li, and P. Ma, ''Characteristic autofluorescence for cancer diagnosis and its origin,'' *Lasers Surg. Med.* **7**, 528–532 (1987).
38. D. M. Harris and J. Werkhaven, ''Endogenous porphyrin fluorescence in tumors,'' *Lasers Surg. Med.* **7**, 467–472 (1987).